THE JOURNAL OF BIOLOGICAL CHEMISTRY
Vol. 279, No. 51, Issue of December 17, pp. 53353–53364, 2004
Printed in U.S.A.

Mcm2 Is a Direct Substrate of ATM and ATR during DNA Damage and DNA Replication Checkpoint Responses*[S]

Received for publication, July 15, 2004, and in revised form, August 30, 2004
Published, JBC Papers in Press, September 22, 2004, DOI 10.1074/jbc.M408026200

Hae Yong Yoo‡, Anna Shevchenko§, Andrej Shevchenko§, and William G. Dunphy‡¶

From the ‡Division of Biology, California Institute of Technology, Pasadena, California 91125 and the §Max Planck Institute of Molecular Cell Biology and Genetics, Pfotenhauerstrasse 108, 01307 Dresden, Germany

In vertebrates, ATM and ATR are critical regulators of checkpoint responses to damaged and incompletely replicated DNA. These checkpoint responses involve the activation of signaling pathways that inhibit the replication of chromosomes with DNA lesions. In this study, we describe the isolation of a cDNA encoding a full-length version of *Xenopus* ATM. Using antibodies against the regulatory domain of ATM, we have identified the essential replication protein Mcm2 as an ATM-binding protein in *Xenopus* egg extracts. *Xenopus* Mcm2 underwent phosphorylation at Ser^{92} in response to the presence of double-stranded DNA breaks or DNA replication blocks in egg extracts. This phosphorylation involved both ATM and ATR, but the relative contribution of each kinase depended upon the checkpoint-inducing DNA signal. Furthermore, both ATM and ATR phosphorylated Mcm2 directly at Ser^{92} in cell-free kinase assays. Immunodepletion of both ATM and ATR abrogated the checkpoint response that blocks chromosomal DNA replication in egg extracts containing double-stranded DNA breaks. These experiments indicate that ATM and ATR phosphorylate the functionally critical replication protein Mcm2 during both DNA damage and replication checkpoint responses in *Xenopus* egg extracts.

In eukaryotic cells, various checkpoint control mechanisms guard the integrity of the genomic DNA throughout the cell cycle (for reviews, see Refs. 1–3). For example, early in the cell cycle, these regulatory pathways block the entry into S phase if the genomic DNA suffers various types of damage. In cells that already have entered S phase, other checkpoint responses act to block further replication by inhibiting elongation at existing forks and by preventing the firing of any new replication origins. Finally, the presence of damaged or incompletely replicated DNA in the cell also prevents the entry into mitosis. These pathways contain sensor proteins that detect various nucleic acid structures and associated proteins at DNA replication forks or sites of DNA damage. The sensor proteins control the activity of effector proteins, which regulate cell cycle processes. A third class of proteins termed mediators or adaptors may facilitate interactions between sensor and effector proteins. Some checkpoint proteins may perform more than one of these functions.

Members of the phosphoinositide kinase-related family of protein kinases function at or near the top of various checkpoint regulatory pathways. In vertebrates, the phosphoinositide kinase-related kinases include ATM and ATR (4). ATM plays a key role in the response of cells to double-stranded DNA breaks, which occur following ionizing radiation and other insults to the genome. On the other hand, ATR is involved in detecting DNA replication forks and any problems that might arise in these critical but transient structures during S phase (5–8). ATM is dispensable for cell viability, but absence of functional ATR is lethal, presumably because of its role in monitoring the success of DNA replication (9, 10). In view of the importance of ATM and ATR to the preservation of genomic integrity, it will be critical to elucidate how these kinases undergo activation during checkpoint responses and to identify their key downstream targets.

One of the important functions of checkpoint pathways regulated by the phosphoinositide kinase-related kinases appears to be control of the DNA replication machinery in the cell (3). The initiation of DNA replication is an elaborate process that involves the sequential recruitment of key replication proteins to future origins of DNA replication (11). Initially, the origin recognition complex recruits Cdc6 and Cdt1 to the DNA. In turn, these proteins allow the loading of the minichromosome maintenance (MCM)[1] complex onto the DNA. Thereafter, this complex enables the binding of various additional proteins, notably Cdc45, to chromatin. The binding of Cdc45 and regulated phosphorylation by the kinases Cdc7 and Cdk2 are rate-limiting steps for the initiation of DNA replication (12). The MCM complex, possibly in conjunction with associated proteins, appears to represent a specific helicase activity that is essential for the replicative unwinding of DNA that begins at newly fired origins. Not surprisingly, the MCM complex appears to be subject to multiple levels of regulation during the cell cycle (reviewed in Refs. 13 and 14).

Xenopus egg extracts have proven to be a valuable tool for functional analysis of checkpoint regulatory pathways. In this system, the addition of the DNA polymerase inhibitor aphidicolin to elicit replication blocks results in the accumulation of incompletely replicated DNA (15, 16). This response results in the activation of Xchk1, the *Xenopus* homolog of the effector kinase Chk1 (16). In this context, the activation of Xchk1 requires the action of *Xenopus* ATR (Xatr) (5, 6). Moreover, DNA damage responses can also be studied in these extracts. In particular, the introduction of DNA with free double-stranded ends, which would mimic damaged DNA, into these

* This work was supported in part by National Institutes of Health Grant GM43974. The costs of publication of this article were defrayed in part by the payment of page charges. This article must therefore be hereby marked "*advertisement*" in accordance with 18 U.S.C. Section 1734 solely to indicate this fact.

[S] The on-line version of this article (available at http://www.jbc.org) contains Supplemental Fig. S1.

The nucleotide sequence(s) reported in this paper has been submitted to the GenBank™/EBI Data Bank with accession number(s) AY668954.

¶ To whom correspondence should be addressed: Div. of Biology, 216-76, 1200 E. California Blvd., California Inst. of Technology, Pasadena, CA 91125. Tel.: 626-395-8433; Fax: 626-795-7563; E-mail: dunphy@cco.caltech.edu.

[1] The abbreviations used are: MCM, minichromosome maintenance; GST, glutathione *S*-transferase.

extracts inhibits both DNA replication and entry into mitosis (17–19). As is the case in human cells, ATM is involved in checkpoint regulation in response to the presence of DNA with exposed double-stranded ends (18).

For this study, we set out to probe the function and regulation of ATM by searching for ATM-interacting proteins in *Xenopus* egg extracts. To initiate these experiments, we isolated a cDNA encoding the full-length version of *Xenopus* ATM (Xatm). Using antibodies against a previously undescribed region from the regulatory domain of Xatm, we identified *Xenopus* Mcm2 (Xmcm2) as a specific binding partner for Xatm. Moreover, we also found that Xmcm2 is a direct and efficient substrate of ATM. Further analyses indicated that Xmcm2 is likewise a specific target of ATR. Therefore, Xmcm2 is a direct target of the two major phosphoinositide kinase-related kinases involved in DNA-regulated checkpoint responses in this system.

EXPERIMENTAL PROCEDURES

Cloning of a cDNA Encoding Full-length Xatm—Poly(A)$^+$ RNA was isolated from *Xenopus* oocyte total RNA and subjected to first strand cDNA synthesis. A *Xenopus* oocyte cDNA library was constructed and ligated with adaptors using the Marathon cDNA amplification kit (Clontech). 5′-Rapid amplification of cDNA ends/PCR was performed using primer 5′-TGCCCACAATGACATGGTGGTGACACTC-3′ based on a sequence in the C-terminal half of Xatm and adaptor primer-1 from the Marathon cDNA kit. After a second PCR using nested primers (5′-GCAACAGATCGAGGCAAAGCAAGAGACTG-3′ and adaptor primer-2 from the Marathon cDNA kit), a 4.6-kb PCR product that encodes the N-terminal half of Xatm was obtained. A 9.2-kb fragment was amplified from the same library using two oligonucleotides (5′-ATGAGTCTTGCGCTACATGAGCTGCTGCTCTGC-3′ and 5′-GCAGAGCAGCAGCTCATGTAGCGCAAGACTCAT-3′) that were designed to span the full-length coding sequence of Xatm. Sequencing of both DNA strands from this fragment revealed an open reading frame of 3061 amino acids.

Antibodies—A DNA fragment encoding amino acids 634–878 of Xatm was produced by PCR and cloned into a pET-His_6 expression vector. The His_6-Xatm-(634–878) protein was expressed in *Escherichia coli*, isolated on nickel-agarose, and used for production of antibodies at a commercial facility. These antibodies recognized the 350-kDa Xatm protein in *Xenopus* egg extracts by both immunoprecipitation and immunoblotting. An anti-human BM28 monoclonal antibody, which recognizes Xmcm2, was purchased from Cell Signaling Technology. Control rabbit IgG was obtained from Zymed Laboratories Inc.. For anti-phospho-Ser^{92} antibodies against phosphorylated Xmcm2, the peptide CEDLTASQREAA (containing residues 87–97) was synthesized with a phosphate at Ser^{92} and an extra cysteine residue for conjugation to keyhole limpet hemocyanin. Anti-phosphopeptide antibodies were prepared as described (20). Affinity-purified antibodies against Xatr, Xchk2, Xchk1, and Xorc2 were as described previously (16, 17, 21, 22). Antisera against Xmcm4 and Xmcm7 were the generous gift of Dr. J. J. Blow (University of Dundee) (23).

Xenopus Egg Extracts—*Xenopus* egg extracts were prepared as described (21). Extracts were treated with 50 μg/ml $(dA)_{70}$-$(dT)_{70}$ to induce checkpoint responses as described (21). To prepare extracts containing chromatin with double-stranded DNA breaks or DNA replication blocks, demembranated sperm nuclei (1000–3000/μl) were incubated in extracts containing 0.05 unit/μl EcoRI or 100 μg/ml aphidicolin, respectively. Caffeine was added at a final concentration of 5 mM to override checkpoint responses (5, 16).

Immunoprecipitation and Immunodepletion—For immunoprecipitations, extracts (100 μl) were incubated with protein A-conjugated magnetic beads (Dynal, Inc.) containing anti-Xatm antibodies (5 μg) or with protein G-conjugated magnetic beads containing anti-BM28 antibodies (5 μg) for 45 min at 4 °C. The beads were washed three times with 10 mM HEPES-KOH (pH 7.5), 150 mM NaCl, 0.5% Nonidet P-40, 2.5 mM EGTA, and 20 mM β-glycerol phosphate and once with HEPES-buffered saline (10 mM HEPES-KOH (pH 7.5) and 150 mM NaCl) and subjected to SDS-PAGE and immunoblotting. For immunodepletion of Xatm, interphase extracts (100 μl) were incubated with 30 μg of anti-Xatm antibodies bound to 120 μl of protein A-conjugated magnetic beads at 4 °C for 45 min. The same amount of control rabbit IgG was used for mock depletion. After the incubation, the beads were removed with a magnet, and the supernatants were treated again for a second round of depletion. Xatr was immunodepleted as described previously (24).

Identification of Xatm-interacting Proteins by Mass Spectrometry—Anti-Xatm immunoprecipitates were subjected to SDS-PAGE and visualized by staining with Coomassie Blue. Protein bands were excised, in gel-digested with trypsin as described previously (25), and analyzed by matrix-assisted laser desorption ionization mass spectrometry on an AnchorChip™ 384–600 target as described (26). The peptide mass fingerprint acquired from the digest of a band at 120 kDa identified the *Xenopus* Mcm2 protein. Ten peptides were matched to its sequence within better than 50 ppm mass tolerance, covering 12% of the protein sequence. A data base search was performed against a non-redundant protein data base (Mass Spectrometry Protein Sequence Database) using Mascot software (Matrix Sciences Ltd., London, United Kingdom). The protein score of the hit was 100 and exceeded the threshold significance score of 74 ($p < 0.05$); and therefore, the identification
was confident.

Kinase Assays—For kinase assays of endogenous Xatm, egg extracts (50 μl) were treated as indicated and then incubated with Affiprep-protein A beads containing anti-Xatm antibodies (3 μg) for 40 min at 4 °C with rotation. The same amount of rabbit IgG was used for control samples. The beads were isolated and washed three times with 80 mM β-glycerol phosphate (pH 7.3), 20 mM EGTA, 15 mM $MgCl_2$, and 1 mM dithiothreitol and twice with HEPES-buffered saline. The beads were resuspended in 50 μl of HEPES-buffered saline. Aliquots (10 μl) were incubated with 1 μg of PHAS-I or GST-Xmcm2 fragment as substrate at room temperature. Wild-type and kinase-inactive versions of recombinant human FLAG-tagged ATM and ATR were produced in 293T cells and assayed for kinase activity as described (27).

Production of Recombinant Proteins in Insect Cells and Bacteria—pFastBac vectors encoding Xmcm2 with GST and His_6 tags at the C-terminal end were derived from the pFastBac-Xchk1-GH vector (21). His_6-tagged versions of Xmcm2 were prepared in the pFastBacHT vector. Recombinant baculoviruses were generated with the Bac-to-Bac system (Invitrogen). Recombinant baculovirus-expressed proteins were produced in Sf9 insect cells and purified using nickel-agarose beads (21). To prepare GST-tagged peptide fragments of Xmcm2, DNA fragments encoding amino acids 62–122, 297–357, 485–545, and 757–817 of Xmcm2 were cloned into a pGEX vector. GST-tagged proteins were produced and purified from bacteria as described (28). Geminin was prepared as described (29). Point mutants in Xmcm2 were produced with the QuikChange kit (Stratagene).

Isolation of Nuclear and Chromatin Fractions—Egg extracts (100–200 μl) containing 3000 sperm nuclei/μl were incubated under the indicated conditions, overlaid on a 1-ml sucrose cushion containing chromatin isolation buffer (20 mM HEPES-KOH (pH 7.6), 1 M sucrose, 80 mM KCl, 25 mM potassium gluconate, and 10 mM magnesium gluconate), and centrifuged at 6100 × *g* for 5 min. The pellets were washed twice with chromatin isolation buffer. After centrifugation, the pellets (nuclear fractions) were boiled in gel sample buffer and subjected to SDS-PAGE. For preparation of chromatin fractions, the pellets were washed once more with chromatin isolation buffer containing 0.5% Nonidet P-40. The supernatant (nuclear soluble fraction) was removed, and the chromatin pellets were processed for SDS-PAGE. To elute proteins from nuclear fractions, nuclear pellets were incubated on ice for 10 min with 10 mM HEPES-KOH (pH 7.6) containing 0.3 M NaCl and 0.5% Nonidet P-40. The samples were centrifuged at 11,700 × *g* for 5 min, and the supernatants were subjected to immunoprecipitation.

Replication Assays—To monitor DNA replication, interphase extracts were incubated with 1000–3000 sperm nuclei/μl and 100 μg/ml cycloheximide in the presence of [α-^{32}P]dATP as described (24).

Cell Culture and Immunofluorescence—After incubation with EcoRI or aphidicolin, extracts were diluted, fixed, and layered on a sucrose cushion, and nuclei were pelleted onto coverslips as described (30, 31). Indirect immunofluorescence was performed using goat anti-mouse IgG conjugated to Alexa 568 (Molecular Probes, Inc.) and goat anti-rabbit IgG conjugated to Alexa 488 for anti-BM28 and anti-phospho-Ser^{92} antibodies, respectively. Chromatin was stained with Hoechst 33258 to visualize the DNA. Samples were viewed on a Zeiss Axioplan fluorescence microscope and imaged with a SpotRT CCD camera (Diagnostic Instruments) at identical magnifications and exposure times.

HeLa cells were treated with γ-irradiation, UV light, or hydroxyurea as indicated. Cells were processed 2 h after treatment with γ-irradiation or UV or 24 h after the addition of hydroxyurea to the culture. For localized UV damage, cells were overlaid with a 3-μm Isopore polycarbonate filter (Millipore) prior to irradiation with 100 J/m^2 UV as described (32) and allowed to recover for 90 min prior to immunostaining. For immunoblotting, whole cell extracts were prepared and subjected to SDS-PAGE. For indirect immunofluorescence, cells were grown on poly-

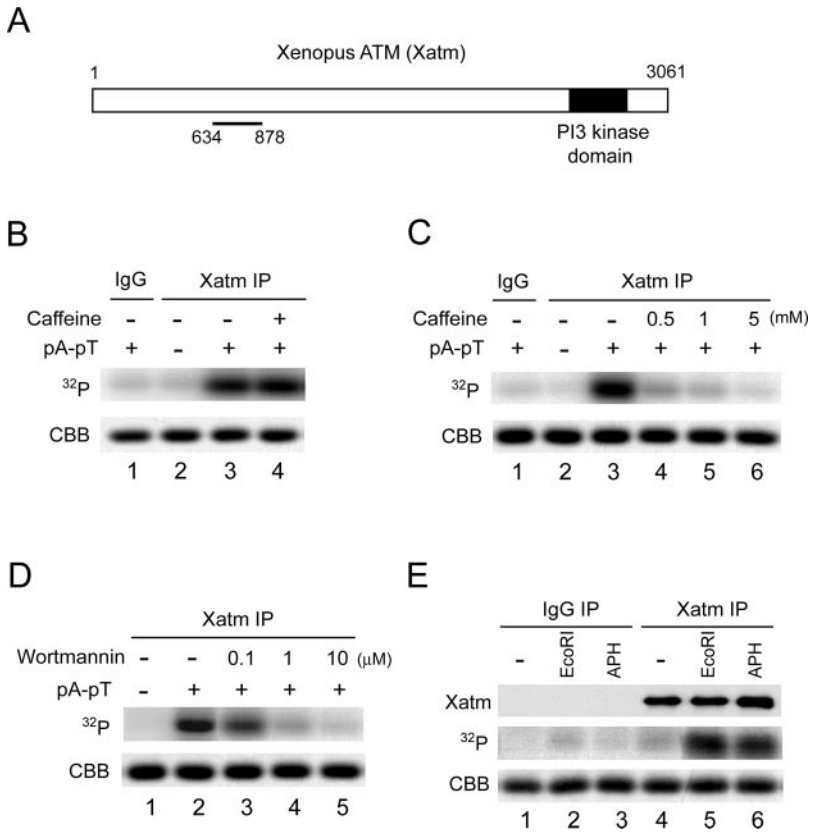

FIG. 1. **Xatm undergoes activation during checkpoint responses in egg extracts.** *A*, diagram of full-length Xatm. The sequence of full-length Xatm contains 3061 amino acids. The phosphoinositide 3-kinase (*PI3 kinase*) domain and the region used for antibody production (amino acids 634–878) are denoted. *B*, Xatm-associated kinase activity. Interphase extracts containing no DNA (*lane 2*), $(dA)_{70}$-$(dT)_{70}$ (*pA-pT*) (*lanes 1* and *3*), or $(dA)_{70}$-$(dT)_{70}$ plus caffeine (*lane 4*) were incubated for 100 min and immunoprecipitated (*IP*) with control IgG (*lane 1*) or anti-Xatm antibodies (*lanes 2–4*). The immunoprecipitates were incubated with PHAS-I as substrate in the presence of [^{32}P]ATP. After SDS-PAGE, PHAS-I was visualized by Coomassie Brilliant Blue (*CBB*) staining (*lower panel*). Incorporation of ^{32}P was detected with a PhosphorImager (*upper panel*). *C*, sensitivity of Xatm-associated kinase activity to caffeine. Kinase assays were performed by incubating control IgG (*lane 1*) or anti-Xatm (*lanes 2–6*) immunoprecipitates from extracts containing no DNA (*lane 2*) or $(dA)_{70}$-$(dT)_{70}$ (*lanes 1* and *3–6*) with PHAS-I and 0–5 mM caffeine as indicated. PHAS-I was stained with Coomassie Blue (*lower panel*), and incorporation of ^{32}P was detected with a PhosphorImager (*upper panel*). *D*, sensitivity of Xatm kinase activity to wortmannin. Anti-Xatm immunoprecipitates from extracts containing $(dA)_{70}$-$(dT)_{70}$ were incubated with PHAS-I and 0–10 μM wortmannin. PHAS-I was stained with Coomassie Blue (*lower panel*), and incorporation of ^{32}P was detected with a PhosphorImager (*upper panel*). *E*, extracts incubated for 100 min with 3000 sperm nuclei/μl alone (*lanes 1* and *4*), sperm nuclei plus EcoRI (*lanes 2* and *5*), or sperm nuclei plus aphidicolin (*APH*) (*lanes 3* and *6*). Nuclear fractions were isolated and extracted with 0.3 M NaCl. The salt eluates were immunoprecipitated with control IgG (*lanes 1–3*) or anti-Xatm antibodies (*lanes 4–6*). The immunoprecipitates were incubated with PHAS-I in the presence of [^{32}P]ATP. PHAS-I was stained with Coomassie Blue (*lower panel*), and incorporation of ^{32}P was detected with a PhosphorImager (*middle panel*). The immunoprecipitates were immunoblotted with anti-Xatm antibodies (*upper panel*).

D-lysine-coated coverslips. After treatment, cells were fixed with 3% paraformaldehyde in phosphate-buffered saline for 30 min, permeabilized with 1% Triton X-100 in phosphate-buffered saline, and processed for microscopy. Mouse anti-BM28 monoclonal and rabbit anti-phospho-Ser^{108} polyclonal antibodies were used as primary antibodies, and either goat anti-mouse IgG conjugated to Alexa 568 or goat anti-rabbit IgG conjugated to Alexa 488 was used as the secondary antibody at 1:250 dilution. TO-PRO-3 iodide (Molecular Probes, Inc.) or Hoechst 33258 was used to detect nuclear DNA. The coverslips were washed, mounted onto glass slides, and viewed with a Leica SP confocal microscope or a Zeiss Axioplan fluorescence microscope.

RESULTS

Cloning of a Full-length Xenopus Homolog of ATM—To study the role of ATM in checkpoint responses in *Xenopus* egg extracts, we isolated a cDNA encoding a full-length homolog of *Xenopus* ATM (Xatm). A fragment containing the C-terminal half of Xatm was described previously (33). To identify the N-terminal region of Xatm, we cloned a 4.8-kb cDNA from a *Xenopus* oocyte Marathon cDNA library by 5′-rapid amplification of cDNA ends. Next, using two primers for the predicted extreme 5′- and 3′-ends of Xatm, we amplified a 9.2-kb fragment from this library. Upon DNA sequencing of this fragment, we identified an open reading frame of 3061 amino acids that encodes the full-length Xatm protein (Fig. 1*A*). An alignment of the N-terminal half of Xatm with human ATM is shown in Supplemental Fig. S1. The predicted amino acid sequence of full-length Xatm shares 64% identity with human ATM. The previously identified kinase domain of Xatm (residues 2676–2981) is 88% identical between the two species, and the N-terminal regulatory domain (residues 1–2676) that has now been fully defined in this study is 61% identical to the corresponding region of human ATM.

Xatm Undergoes Activation in Checkpoint-induced Extracts—Human ATM undergoes activation in response to double-stranded DNA breaks (see Ref. 34). To investigate the regulation of Xatm, we first examined the effect of a defined DNA template with double-stranded DNA ends on Xatm in egg extracts. For this experiment, we utilized annealed oligomers consisting of $(dA)_{70}$ and $(dT)_{70}$. This template ($(dA)_{70}$-$(dT)_{70}$) can induce both DNA damage and DNA replication checkpoint responses effectively in egg extracts (17, 21). We incubated egg extracts with either no DNA or $(dA)_{70}$-$(dT)_{70}$, immunoprecipitated Xatm with anti-Xatm antibodies, and then assayed its kinase activity with PHAS-I as the substrate. As shown in Fig. 1*B*, the activity of Xatm from extracts containing $(dA)_{70}$-$(dT)_{70}$

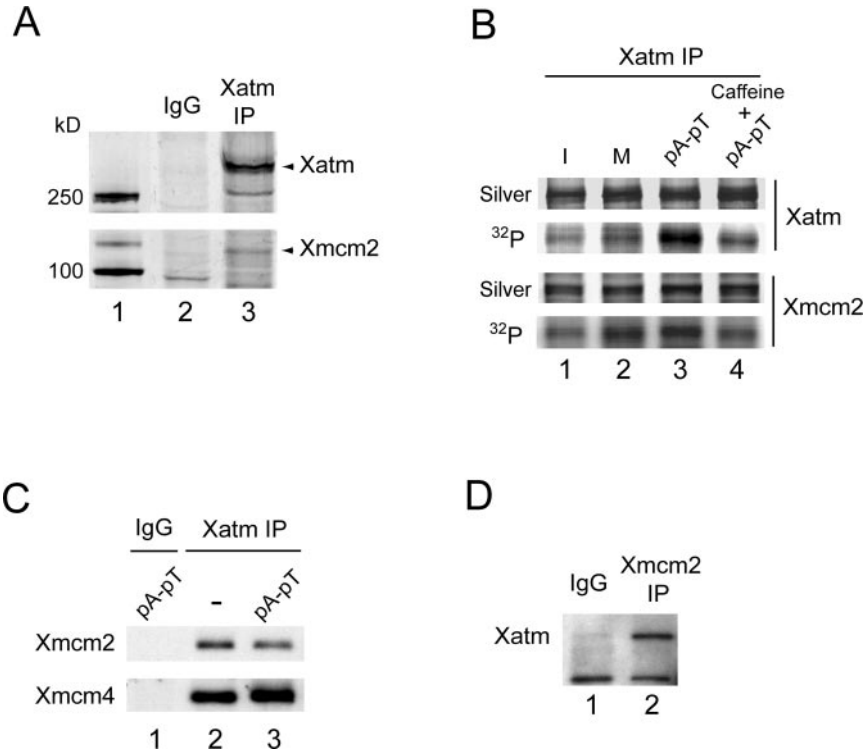

FIG. 2. **Xatm interacts specifically with Xmcm2.** *A*, interphase egg extracts containing $(dA)_{70}$-$(dT)_{70}$ were immunoprecipitated (*IP*) with control IgG (*lane 2*) or anti-Xatm antibodies (*lane 3*). The immunoprecipitates were subjected to SDS-PAGE and silver staining. One band at ~120 kDa (marked with the *arrowhead* in the *lower panel*) was shown to be Xmcm2 by mass spectrometry (see "Experimental Procedures"). The *upper panel* depicts the area of the gel containing Xatm. *Lane 1* shows molecular mass marker proteins. *B*, interphase (*I*) extracts (*lane 1*), M phase (*M*) extracts (*lane 2*), and interphase extracts containing either $(dA)_{70}$-$(dT)_{70}$ (*pA-pT*) (*lane 3*) or $(dA)_{70}$-$(dT)_{70}$ plus caffeine (*lane 4*) were incubated in the presence of [^{32}P]orthophosphate and immunoprecipitated with anti-Xatm antibodies. The immunoprecipitates were subjected to SDS-PAGE. Xatm and Xmcm2 were visualized by silver staining. Incorporation of ^{32}P into Xatm or Xmcm2 was detected with a PhosphorImager. *C*, interphase extracts containing no DNA (*lane 2*) or $(dA)_{70}$-$(dT)_{70}$ (*lanes 1* and *3*) were immunoprecipitated with control IgG (*lane 1*) or anti-Xatm antibodies (*lanes 2* and *3*). Immunoprecipitates were immunoblotted with anti-Xmcm2 and anti-Xmcm4 antibodies. *D*, extracts containing $(dA)_{70}$-$(dT)_{70}$ were immunoprecipitated with control IgG (*lane 1*) or anti-Xmcm2 antibodies (*lane 2*). Immunoprecipitates were immunoblotted with anti-Xatm antibodies.

was much higher than from extracts lacking DNA. Immunoprecipitates with control IgG contained negligible kinase activity.

Caffeine is a well documented inhibitor of phosphoinositide kinase-related kinases such as ATM and ATR (4). To examine whether caffeine affects the activation of Xatm, we immunoprecipitated Xatm from extracts treated with $(dA)_{70}$-$(dT)_{70}$ in the absence or presence of caffeine and then assayed its kinase activity in the absence of caffeine. Interestingly, we found that Xatm underwent activation in both the absence and presence of caffeine (Fig. 1*B*). To confirm that Xatm is indeed sensitive to caffeine, we assayed its kinase activity in the presence of various concentrations of this compound. We observed that the kinase activity of the activated form of Xatm was totally suppressed when caffeine was present at a concentration of 0.5 mM or higher in the kinase assay incubation (Fig. 1*C*). We also found that Xatm was completely inhibited by 1 μM wortmannin (Fig. 1*D*), as is the case for human ATM (35). Overall, these results indicate that Xatm, like human ATM, is sensitive to caffeine and wortmannin. However, the process leading to the activation of Xatm can still occur in the presence of caffeine. It has recently been proposed that the activation of human ATM involves intermolecular autophosphorylation of inactive ATM dimers (34). One possibility is that the autophosphorylation activity of ATM is less sensitive to caffeine. Another scenario is that the activation of ATM can occur without autophosphorylation under some circumstances. Finally, since we need to assay activated Xatm in the absence of caffeine, it is possible that there is some caffeine-insensitive step upstream of autophosphorylation that is involved in the activation of ATM.

Next, we examined the regulation of Xatm in response to lesions in chromosomal DNA. For this purpose, we added demembranated sperm chromatin to egg extracts to initiate the formation of reconstituted nuclei. We introduced double-stranded DNA breaks into the chromosomal DNA by including the restriction endonuclease EcoRI in the extracts (19). Moreover, we induced the formation of stalled replication forks in the chromatin by adding the DNA polymerase inhibitor aphidicolin. After 100 min, we isolated nuclear fractions from the incubations, extracted nuclear proteins with 0.3 M NaCl, and then immunoprecipitated the salt eluates with control or anti-Xatm antibodies. We observed that the activity of Xatm for PHAS-I increased in response to treatment with either EcoRI or aphidicolin (Fig. 1*E*). Similar amounts of Xatm protein were immunoprecipitated under all conditions. These results demonstrate that both double-stranded DNA breaks and replication blocks can elicit the activation of Xatm in egg extracts.

Xatm Interacts Specifically with Xmcm2—The identification of ATM-interacting proteins could help to elucidate upstream and downstream regulators of ATM-dependent checkpoint responses. We searched for Xatm-interacting proteins by immunoprecipitating Xatm from *Xenopus* egg extracts with anti-Xatm antibodies and silver staining the immunoprecipitates (Fig. 2*A*). Our interest was attracted by a band at ~120 kDa because ^{32}P labeling experiments indicated that this protein underwent cell cycle-regulated and checkpoint-dependent phosphorylation (Fig. 2*B*). In particular, the 120-kDa band was significantly phosphorylated in interphase egg extracts. This phosphorylation increased in both M phase extracts and interphase extracts containing $(dA)_{70}$-$(dT)_{70}$. The elevated phospho-

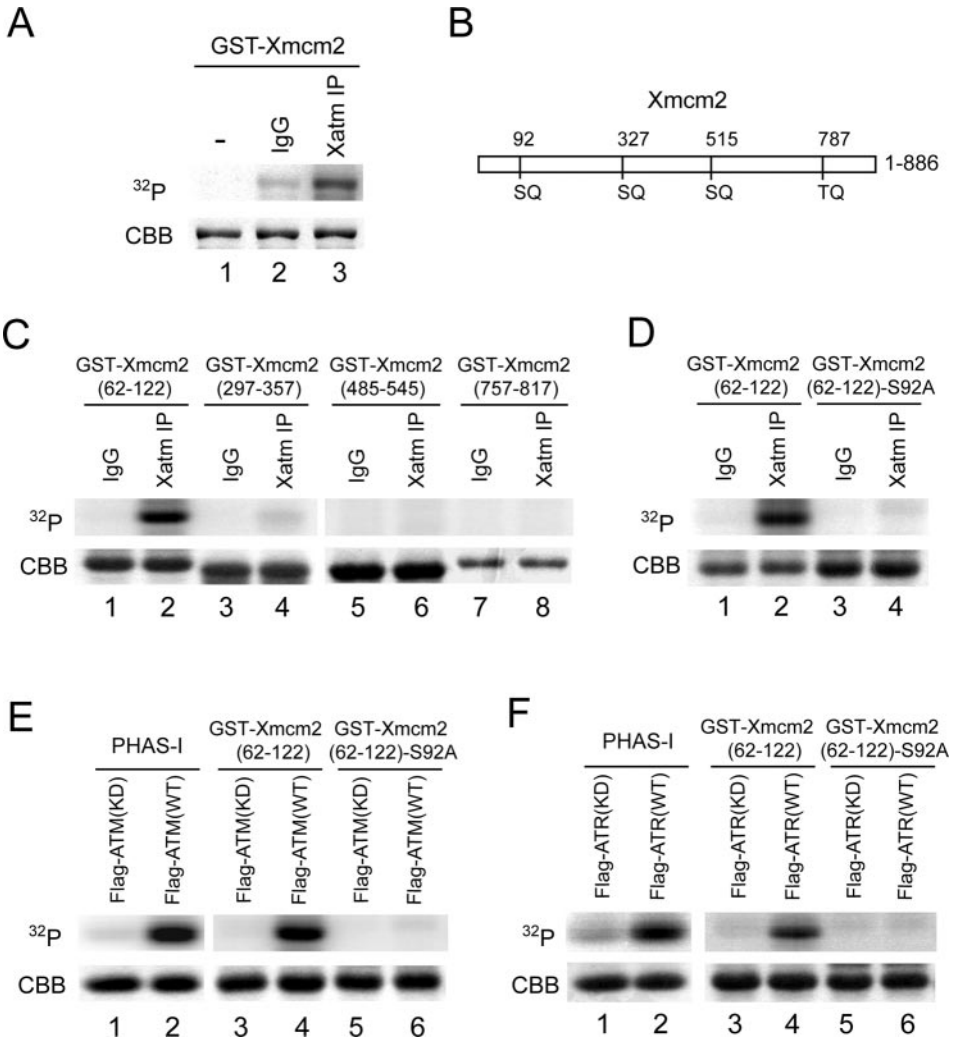

FIG. 3. **ATM and ATR phosphorylate Xmcm2 at Ser^{92}.** *A*, GST-Xmcm2 was incubated in the presence of [^{32}P]ATP with no immunoprecipitates (*lane 1*) or either control immunoprecipitates (*lane 2*) or anti-Xatm immunoprecipitates (*IP*) (*lane 3*) from extracts containing $(dA)_{70}$-$(dT)_{70}$. The samples were subjected to SDS-PAGE. GST-Xmcm2 protein was visualized by Coomassie Brilliant Blue (*CBB*) staining (*lower panel*). Incorporation of ^{32}P was detected with a PhosphorImager (*upper panel*). *B*, shown is a diagram of SQ/TQ motifs in Xmcm2. *C*, GST-Xmcm2-(62–122) (*lanes 1* and *2*), GST-Xmcm2-(297–357) (*lanes 3* and *4*), GST-Xmcm2-(485–545) (*lanes 5* and *6*), and GST-Xmcm2-(757–817) (*lanes 7* and *8*) were incubated with [^{32}P]ATP and either control IgG (*lanes 1*, *3*, *5*, and *7*) or anti-Xatm (*lanes 2*, *4*, *6*, and *8*) immunoprecipitates from extracts containing $(dA)_{70}$-$(dT)_{70}$. After SDS-PAGE, GST-tagged fragments were visualized by Coomassie Blue staining (*lower panel*). Incorporation of ^{32}P into these fragments was detected with a PhosphorImager (*upper panel*). *D*, GST-Xmcm2-(62–122) (*lanes 1* and *2*) and GST-Xmcm2-(62–122)(S92A) (*lanes 3* and *4*) were incubated in the presence of [^{32}P]ATP with control immunoprecipitates (*lanes 1* and *3*) or anti-Xatm immunoprecipitates from extracts containing $(dA)_{70}$-$(dT)_{70}$ (*lanes 2* and *4*). The samples were subjected to SDS-PAGE. GST-Xmcm2 fragments were stained with Coomassie Blue (*lower panel*). Incorporation of ^{32}P was detected with a PhosphorImager (*upper panel*). *E* and *F*, human ATM and ATR phosphorylated Xmcm2 at Ser^{92}. Wild-type (*WT*) or kinase-inactive (*KD*) FLAG-ATM and FLAG-ATR were isolated from 293T cells as described under "Experimental Procedures." For *E*, PHAS-I (*lanes 1* and *2*), GST-Xmcm2-(62–122) (*lanes 3* and *4*), and GST-Xmcm2-(62–122)(S92A) (*lanes 5* and *6*) were incubated in the presence of [^{32}P]ATP with kinase-inactive FLAG-ATM (*lanes 1*, *3*, and *5*) and wild-type FLAG-ATM (*lanes 2*, *4*, and *6*). For *F*, kinase-inactive FLAG-ATR (*lanes 1*, *3*, and *5*) and wild-type FLAG-ATR (*lanes 2*, *4*, and *6*) were used in the kinase reactions. The samples were subjected to SDS-PAGE. PHAS-I and GST-tagged Xmcm2 fragments were visualized by Coomassie Blue staining (*lower panel*), and incorporation of ^{32}P was detected with a PhosphorImager (*upper panel*).

rylation in the presence of $(dA)_{70}$-$(dT)_{70}$ was reversed by caffeine. By comparison, Xatm displayed similar phosphorylation during interphase and M phase, but its phosphorylation also increased in interphase extracts containing $(dA)_{70}$-$(dT)_{70}$. This phosphorylation was likewise prevented by the addition of caffeine. Mass spectrometric analysis of a large-scale anti-Xatm immunoprecipitate from interphase egg extracts, which was stained with Coomassie Blue in this case, indicated that the 120-kDa band corresponds to Xmcm2 (see "Experimental Procedures").

To evaluate the specificity of the interaction between Xatm and Xmcm2, we carried out reciprocal immunoprecipitation experiments. First, we immunoprecipitated Xatm from interphase egg extracts either lacking or containing $(dA)_{70}$-$(dT)_{70}$ and then performed immunoblotting with anti-Xmcm2 antibodies. We observed that Xmcm2 could be found in similar amounts in the anti-Xatm immunoprecipitates from extracts that had been incubated in the absence or presence of $(dA)_{70}$-$(dT)_{70}$ (Fig. 2*C*). We also detected Xmcm4 (Fig. 2*C*) and Xmcm7 (data not shown) in these immunoprecipitates by immunoblotting, suggesting that the entire MCM complex was isolated with the anti-Xatm antibodies. Furthermore, we also detected Xatm in anti-Xmcm2 immunoprecipitates by immunoblotting with anti-Xatm antibodies (Fig. 2*D*). These findings indicate that Xatm and Xmcm2 form a specific complex in egg extracts.

Identification of a Phosphorylation Site on Xmcm2 for Xatm—Because kinases often form complexes with their substrates, we asked whether Xmcm2 could serve as a substrate

for Xatm. As shown in Fig. 3*A*, full-length GST-Xmcm2 underwent efficient phosphorylation upon incubation with [^{32}P]ATP and anti-Xatm immunoprecipitates from $(dA)_{70}$-$(dT)_{70}$-containing extracts, but not with control immunoprecipitates from such extracts. It is known that ATM, ATR, and the DNA-dependent protein kinase display a preference to phosphorylate SQ or TQ motifs in their substrates (36). Xmcm2 contains three SQ motifs (Ser^{92}, Ser^{327}, and Ser^{515}) and one TQ motif (Thr^{787}) (Fig. 3*B*). To assess whether Xatm could phosphorylate these sites, we prepared bacterially expressed GST fusion peptides containing amino acids 62–122, 297–357, 485–545, and 757–817 of Xmcm2. Each GST peptide was designed to contain one SQ/TQ motif. We observed that GST-Xmcm2-(62–122) served as an excellent substrate for immunoprecipitated Xatm (Fig. 3*C*). By contrast, the other three GST-Xmcm2 peptides did not become phosphorylated in this assay. To evaluate whether Ser^{92} is the phosphorylated site in GST-Xmcm2-(62–122), we prepared a version of GST-Xmcm2-(62–122) in which this residue was changed to alanine. As shown in Fig. 3*D*, GST-Xmcm2-(62–122)(S92A) could not serve as a substrate for Xatm.

To characterize these observations further, we asked whether recombinant ATM could also phosphorylate Xmcm2. We were unable to produce full-length His_6-Xatm in baculovirus-infected insect cells (data not shown). Therefore, we used recombinant human FLAG-tagged ATM that had been expressed in human 293T cells for these experiments. We found that wild-type FLAG-ATM could phosphorylate the GST-Xmcm2-(62–122) substrate as efficiently as PHAS-I (Fig. 3*E*). As a control, we showed that kinase-inactive FLAG-ATM could not phosphorylate either GST-Xmcm2-(62–122) or PHAS-I in these assays. Consistent with the results described for immunoprecipitated Xatm, human FLAG-ATM did not phosphorylate the GST-Xmcm2-(62–122)(S92A) peptide.

Because ATM and ATR share related substrate specificities, we also asked whether Ser^{92} of Xmcm2 could serve as a substrate for ATR. To test this possibility, we performed kinase assays using wild-type and kinase-inactive recombinant human FLAG-ATR, both of which were also expressed in 293T cells. As shown in Fig. 3*F*, wild-type FLAG-ATR, but not kinase-inactive FLAG-ATR, also phosphorylated GST-Xmcm2-(62–122) efficiently. The S92A mutant of this peptide was not phosphorylated by FLAG-ATR in these assays.

Phosphorylation of Xmcm2 at Ser^{92} Is Checkpoint-regulated—Next, we examined whether Ser^{92} of Xmcm2 undergoes phosphorylation in egg extracts. As one means to address this issue, we incubated GST-Xmcm2-(62–122) and GST-Xmcm2-(62–122)(S92A) in egg extracts containing [^{32}P]orthophosphate in the presence and absence of $(dA)_{70}$-$(dT)_{70}$. As depicted in Fig. 4*A*, GST-Xmcm2-(62–122) became efficiently labeled with ^{32}P in the presence of $(dA)_{70}$-$(dT)_{70}$, but not in its absence. There was no labeling of the S92A mutant polypeptide in these experiments.

To establish directly that Ser^{92} undergoes phosphorylation in egg extracts, we prepared antibodies against a synthetic peptide from a region of Xmcm2 that contains phosphorylated Ser^{92} (anti-phospho-Ser^{92} antibodies). The anti-phospho-Ser^{92} antibodies reacted well with GST-Xmcm2-(62–122) in extracts that had been incubated in the presence of $(dA)_{70}$-$(dT)_{70}$, but not in its absence (Fig. 4*B*). The anti-phospho-Ser^{92} antibodies did not recognize the GST-Xmcm2-(62–122)(S92A) mutant polypeptide under any conditions (Fig. 4*B*). We also examined the endogenous Xmcm2 protein in similar experiments. The anti-phospho-Ser^{92} antibodies could likewise detect phosphorylation of endogenous Xmcm2 in egg extracts in response to $(dA)_{70}$-$(dT)_{70}$ (Fig. 4*C*). This phosphorylation was substantially reduced upon the addition of caffeine.

To examine the effect of lesions in chromosomal DNA on the phosphorylation of Xmcm2 at Ser^{92}, we introduced double-stranded breaks or caused the formation of stalled replication forks by adding EcoRI or aphidicolin, respectively, to egg extracts containing sperm chromatin. After 100 min of incubation, we isolated chromatin fractions from the extracts and performed immunoblotting with antibodies against Xmcm2, phospho-Ser^{92} of Xmcm2, and Xorc2 (to follow recovery of chromatin) (Fig. 4*D*). We observed that Xmcm2 could be found in elevated amounts on both EcoRI-damaged and aphidicolin-treated chromatin. Xmcm2 that had associated with chromatin in extracts treated with EcoRI or aphidicolin reacted strongly with the anti-phospho-Ser^{92} antibodies. By contrast, Xmcm2 that remained in nuclear soluble fractions from these extracts was only weakly phosphorylated at Ser^{92}. We observed that Ser^{92} of Xmcm2 likewise was phosphorylated on chromatin containing UV damage, which also creates DNA replication blocks (data not shown). Finally, chromatin-bound Xmcm2 from control extracts lacking EcoRI or aphidicolin did not react with the anti-phospho-Ser^{92} antibodies.

We also examined time courses for the phosphorylation of Xmcm2 at Ser^{92} under the various conditions described above (Fig. 4*E*). In control egg extracts, the binding of Xmcm2 to chromatin typically began in 5–10 min, peaked at 60–80 min, and then declined by 120 min as DNA replication approached completion (data not shown). In extracts treated with EcoRI and aphidicolin, Xmcm2 bound in elevated amounts to chromatin, and the binding persisted until at least 150 min. In both cases, the phosphorylation of Xmcm2 at Ser^{92} commenced at ~40 min, which coincides with the timing that DNA replication would normally undergo initiation in untreated extracts.

To characterize further the phosphorylation of Xmcm2 at Ser^{92}, we performed indirect immunofluorescence studies. For this purpose, we used anti-Xmcm2 and anti-phospho-Ser^{92} antibodies for immunostaining nuclei that were isolated from egg extracts (Fig. 4*F*). By this procedure, we could readily detect the Xmcm2 protein in nuclei from control extracts as well as in nuclei from extracts that were treated with EcoRI or aphidicolin. By contrast, the anti-phospho-Ser^{92} antibodies reacted only with EcoRI- and aphidicolin-treated nuclei. In all cases, the anti-Xmcm2 antibodies yielded a diffuse staining pattern that largely coincided with the DNA, consistent with previous findings in various organisms. By contrast, the staining with the anti-phospho-Ser^{92} antibodies in nuclei containing incompletely replicated or damaged DNA was more punctate. Taken together, these experiments indicate that the anti-phospho-Ser^{92} antibodies are useful for detecting the checkpoint-dependent phosphorylation of Mcm2 by both immunoblotting and indirect immunofluorescence.

Human MCM2 Undergoes Phosphorylation at Ser^{108} in Response to Genotoxic Stress—To investigate whether the phosphorylation of MCM2 during checkpoint responses is conserved in mammalian cells, we examined HeLa cells that were subjected to a variety of genotoxic stresses. The amino acid sequence around the S92Q motif of Xmcm2 is well conserved in both human and mouse MCM2 (Fig. 5*D*). Therefore, it seemed likely that the anti-phospho-Ser^{92} antibodies directed against phosphorylated Xmcm2 could detect the phosphorylation of the corresponding serine (Ser^{108}) in human MCM2. We exposed exponentially growing HeLa cells to γ-irradiation (2.5–10 gray), ultraviolet light (50–200 J/m^2), or hydroxyurea (0.5–2 mM). After 2 h in the cases of the γ-irradiation and UV treatments or after 24 h for the hydroxyurea treatment, we prepared lysates from the cells and performed immunoblotting with anti-MCM2 protein and anti-phosphorylated MCM2 antibodies. We found that human MCM2 was well phosphorylated

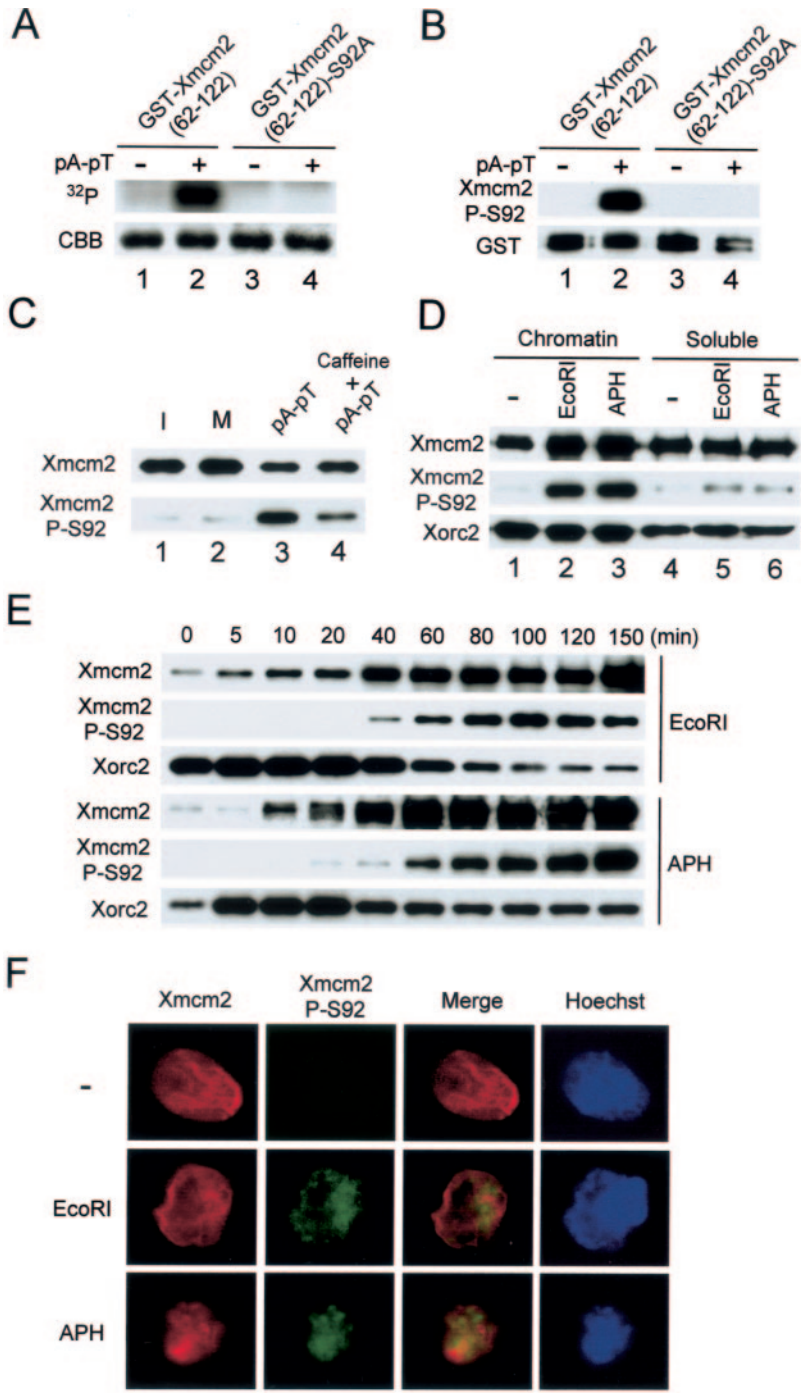

FIG. 4. **Phosphorylation of Xmcm2 at Ser^{92} is induced by double-stranded DNA breaks and replication blocks.** *A*, phosphorylation of Xmcm2 at Ser^{92} was induced by the addition of $(dA)_{70}$-$(dT)_{70}$ to egg extracts. GST-Xmcm2-(62–122) and GST-Xmcm2-(62–122)(S92A) were incubated in egg extracts containing [^{32}P]orthophosphate in the absence (*lanes 1* and *3*) or presence (*lanes 2* and *4*) of $(dA)_{70}$-$(dT)_{70}$ (*pA-pT*). GST-Xmcm2 fragments were re-isolated with glutathione-agarose beads, subjected to SDS-PAGE, and stained with Coomassie Brilliant Blue (*CBB*) (*lower panel*). Incorporation of ^{32}P was detected with a PhosphorImager (*upper panel*). *B*, shown is the specificity of anti-phospho-Ser^{92} antibodies. Interphase extracts containing no DNA (*lanes 1* and *3*) or $(dA)_{70}$-$(dT)_{70}$ (*lanes 2* and *4*) were incubated with GST-Xmcm2-(62–122) (*lanes 1* and *2*) or GST-Xmcm2-(62–122)(S92A) (*lanes 3* and *4*). The GST-tagged Xmcm2 fragments were re-isolated with glutathione-agarose and subjected to SDS-PAGE. The fragments were probed by immunoblotting with anti-phospho-Ser^{92} (*P-S92*) (*upper panel*) or anti-GST (*lower panel*) antibodies. *C*, phosphorylation of endogenous Xmcm2 at Ser^{92} was induced by $(dA)_{70}$-$(dT)_{70}$. Interphase (*I*) extracts (*lane 1*), M phase (*M*) extracts (*lane 2*), and interphase extracts containing $(dA)_{70}$-$(dT)_{70}$ (*lane 3*) or $(dA)_{70}$-$(dT)_{70}$ plus caffeine (*lane 4*) were incubated for 100 min and subsequently subjected to SDS-PAGE. Xmcm2 was probed by immunoblotting with anti-Xmcm2 (*upper panel*) and anti-phospho-Ser^{92} (*lower panel*) antibodies. *D*, extracts were incubated for 100 min with 3000 sperm nuclei/μl alone (*lanes 1* and *4*), sperm nuclei plus EcoRI (*lanes 2* and *5*), or sperm nuclei plus aphidicolin (*APH*) (*lanes 3* and *6*). Chromatin fractions (*lanes 1–3*) and nuclear soluble fractions (*lanes 4–6*) were isolated and immunoblotted with anti-Xmcm2 (*upper panel*), anti-phospho-Ser^{92} (*middle panel*), and anti-Xorc2 (*lower panel*) antibodies. Xorc2 served as a loading control for the chromatin fractions. *E*, chromatin fractions were isolated at the times shown from extracts containing EcoRI or aphidicolin and probed by immunoblotting with anti-Xmcm2, anti-phospho-Ser^{92}, and anti-Xorc2 antibodies as indicated. *F*, shown is the immunostaining of reconstituted sperm nuclei with anti-Xmcm2 and anti-phospho-Ser^{92} antibodies. Sperm nuclei were incubated in mock-treated extracts (*upper row*) or in extracts treated with either EcoRI (*middle row*) or aphidicolin (*lower row*). Nuclei were stained with anti-Xmcm2 and anti-phospho-Ser^{92} antibodies as indicated. DNA was visualized with Hoechst 33258.

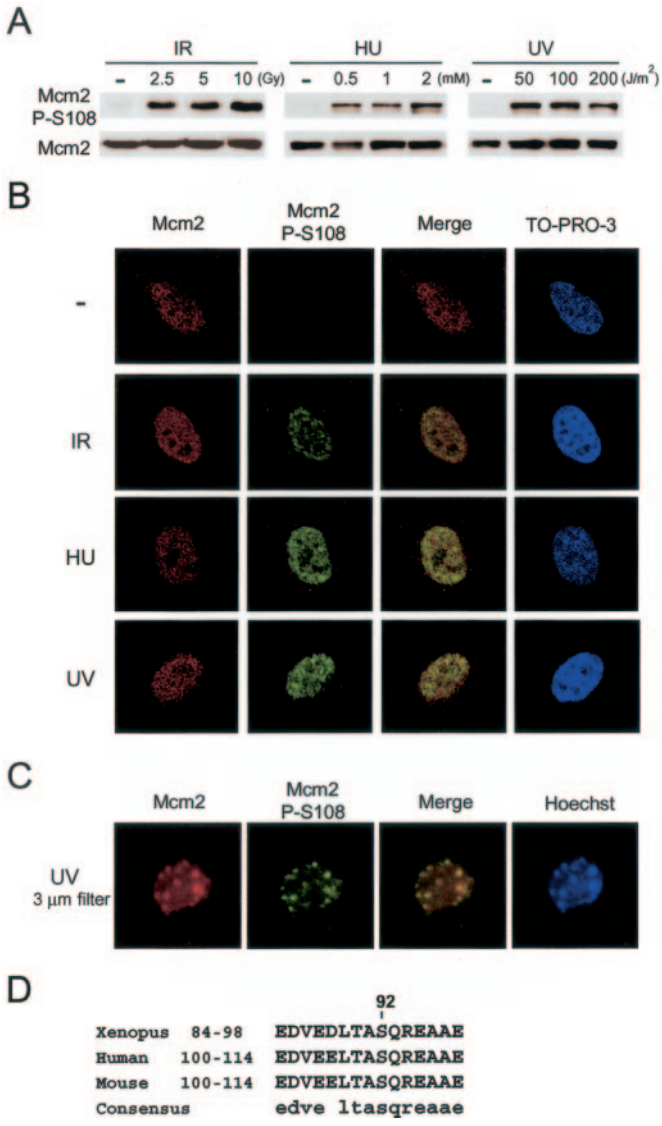

FIG. 5. **Phosphorylation of human MCM2 at Ser^{108} by DNA damage and subcellular localization of MCM2.** *A*, HeLa cells were mock-treated or treated as indicated with γ-irradiation (*IR*), hydroxyurea (*HU*), or ultraviolet light (*UV*). Cell extracts were prepared 2 h after treatment with γ-irradiation or UV light or 24 h after the addition of hydroxyurea, subjected to SDS-PAGE, and immunoblotted with anti-MCM2 (BM28) antibodies and anti-phospho-Ser^{108} (*P-S108*) antibodies. *B*, shown is the subcellular localization of MCM2 and phosphorylated MCM2 in HeLa cells. Cells were fixed after treatment with γ-irradiation (5 gray), hydroxyurea (1 mM), or UV light (100 J/m^2); immunostained with anti-MCM2 and anti-phospho-Ser^{108} antibodies; and viewed under a confocal microscope. Nuclei were visualized by staining with TO-PRO-3 iodide. *C*, HeLa cells were overlaid with a 3-μm Isopore polycarbonate filter, irradiated with 100 J/m^2 UV light, and allowed to recover for 90 min. Cells were stained with anti-MCM2 antibodies, anti-phospho-Ser^{108} antibodies, and Hoechst DNA dye before visualization by fluorescence microscopy. *D*, shown is the alignment of residues 84–98 from *Xenopus* Mcm2 with the corresponding segments of human and mouse MCM2.

at Ser^{108} in response to γ-irradiation, UV light, and hydroxyurea at all doses tested (Fig. 5*A*). For γ-irradiation treatment, phosphorylation was maximal at dose of 10 gray. A concentration of 2 mM hydroxyurea elicited the highest phosphorylation of Ser^{108}, and the level of phosphorylation of this residue was similar at doses of UV light ranging from 50 to 200 J/m^2. By contrast, there was no phosphorylation of Ser^{108} in mock-treated cells that had not been exposed to genotoxic stress.

We also examined the subcellular localization of MCM2 and phosphorylated MCM2 in HeLa cells following genotoxic stress. After treatment with γ-irradiation, hydroxyurea, or UV light, we visualized MCM2 and Ser^{108}-phosphorylated MCM2 by indirect immunofluorescence (Fig. 5*B*). Consistent with the immunoblotting analysis, phosphorylated MCM2 could be detected in cells treated with γ-irradiation, hydroxyurea, and UV light, but not in mock-treated cells. As was the case in *Xenopus* sperm nuclei, the antibodies against phosphorylated MCM2 yielded a punctate staining pattern. To pursue these observations further, we generated localized UV damage in HeLa cell nuclei by overlaying the cells with a 3-μm Isopore polycarbonate filter prior to irradiation. We observed that this treatment resulted in a highly punctate staining pattern with the anti-phospho-Ser^{108} antibodies (Fig. 5*C*). Interestingly, there was also some accumulation of the MCM2 protein in these regions as well. Taken together, these findings indicate that phosphorylation of a conserved serine in MCM2 (*e.g.* Ser^{92} in *Xenopus* and Ser^{108} in humans) is a reliable marker for checkpoint activation in vertebrate cells.

Phosphorylation of Xmcm2 at Ser^{92} Is Dependent on Xatm and Xatr in Egg Extracts—Next, we examined the involvement of Xatm and Xatr in the phosphorylation of Xmcm2 at Ser^{92} in egg extracts. For this purpose, we removed Xatm, Xatr, or both Xatm and Xatr from the extracts by immunodepletion (Fig. 6*A*). First, we examined the phosphorylation of Xmcm2 at Ser^{92} by ^{32}P labeling. GST-Xmcm2-(62–122) was incubated in the various depleted extracts containing [^{32}P]orthophosphate in the presence of $(dA)_{70}$-$(dT)_{70}$ (Fig. 6*B*). The phosphorylation of Ser^{92} in Xatm-depleted extracts was reduced to ~50% in comparison with that in mock-depleted extracts. Furthermore, the phosphorylation of Ser^{92} in extracts lacking both Xatm and Xatr was reduced to ~20% of the mock-depleted value. We observed a similarly reduced level of phosphorylation of Ser^{92} in caffeine-treated extracts. These results suggest that Xatm plays a more prominent role than Xatr in phosphorylation of Ser^{92} in response to $(dA)_{70}$-$(dT)_{70}$.

We also used anti-phospho-Ser^{92} antibodies to assess the involvement of Xatm and Xatr in the checkpoint-dependent phosphorylation of Mcm2 (Fig. 6*C*). In addition to the response to $(dA)_{70}$-$(dT)_{70}$, we also examined how removal of Xatm and Xatr affects the responses to treatment with EcoRI or aphidicolin. For extracts treated with $(dA)_{70}$-$(dT)_{70}$, the removal of Xatm led to a greater reduction in the staining of Xmcm2 with the anti-phospho-Ser^{92} antibodies than removal of Xatr, consistent with the ^{32}P labeling studies described above. In the case of EcoRI-treated extracts, the removal of Xatm likewise had a greater effect, and depletion of both Xatm and Xatr led to a reduction of Ser^{92} phosphorylation similar to that observed following treatment with caffeine. Finally, in aphidicolin-treated extracts, depletion of Xatr caused a greater reduction of Ser^{92} phosphorylation, but removal of Xatm also had a significant impact. Furthermore, absence of both Xatm and Xatr resulted in a level of Ser^{92} phosphorylation comparable with that in caffeine-treated extracts. Taken together, these results indicate that both Xatm and Xatr participate in the checkpoint-dependent phosphorylation of Xmcm2 at Ser^{92}, but that the relative contribution of either kinase depends on the checkpoint-triggering signal.

Xatm and Xatr Cooperatively Inhibit DNA Replication in Response to Double-stranded DNA Breaks—To assess the potential physiological role of the checkpoint-dependent phosphorylation of Xmcm2, we examined the effects of double-stranded DNA breaks on cell cycle progression and DNA replication in egg extracts. As reported previously (19), the restriction endonuclease EcoRI can be used to introduce double-stranded DNA breaks into sperm chromatin in *Xenopus* egg extracts. As shown in Fig. 7*A*, the entry into mitosis occurred after 90–120

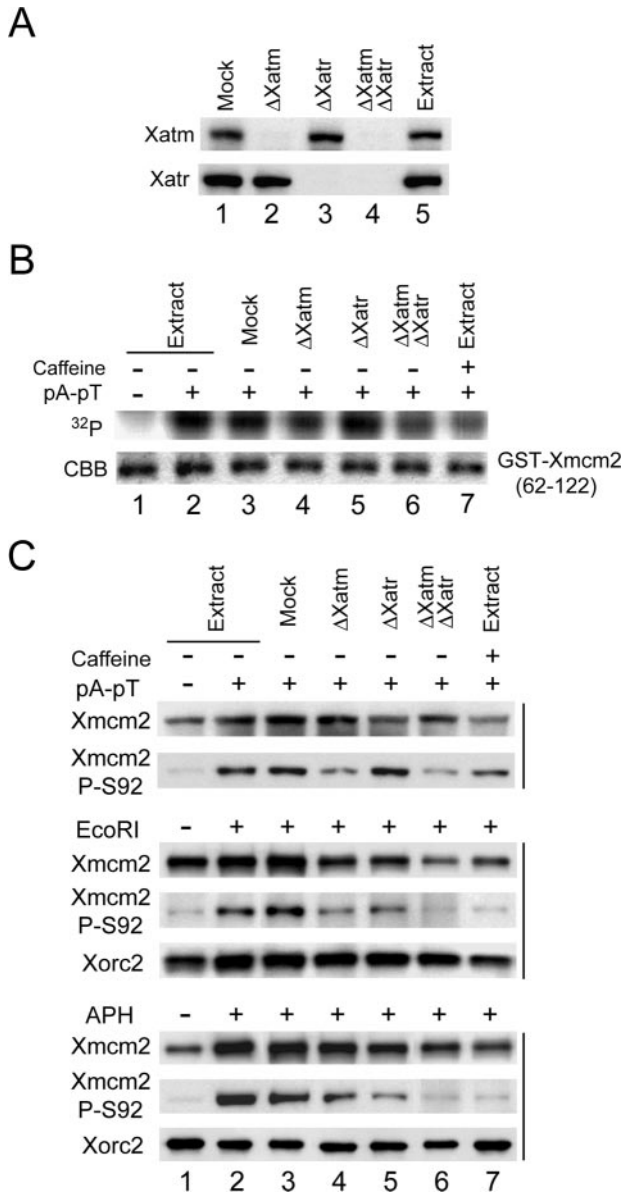

FIG. 6. **Xatm and Xatr phosphorylate Xmcm2 at Ser^{92}.** *A*, shown is the immunodepletion of Xatm (Δ*Xatm*), Xatr (Δ*Xatr*), or both Xatm and Xatr. Extracts were mock-treated (mock immunodepletion with control IgG) (*lane 1*) or treated with anti-Xatm antibodies (*lane 2*), anti-Xatr antibodies (*lane 3*), or both anti-Xatm and anti-Xatr antibodies (*lane 4*) and processed for immunoblotting with anti-Xatm (*upper panel*) or anti-Xatr (*lower panel*) antibodies. *Lane 5* depicts untreated extract. *B*, phosphorylation of GST-Xmcm2-(62–122) at Ser^{92} in the presence of $(dA)_{70}$-$(dT)_{70}$ was dependent on Xatm and Xatr. Untreated extracts (*lanes 1*, *2*, and *7*), mock-depleted extracts (*lane 3*), Xatm-depleted extracts (*lane 4*), Xatr-depleted extracts (*lane 5*), and Xatm- and Xatr-depleted extracts (*lane 6*) were incubated with GST-Xmcm2-(62–122) in the presence of no DNA (*lane 1*), $(dA)_{70}$-$(dT)_{70}$ (*pA-pT*) (*lanes 2–6*), or $(dA)_{70}$-$(dT)_{70}$ plus caffeine (*lane 7*). All extracts contained [^{32}P]orthophosphate. GST-Xmcm2-(62–122) was re-isolated with glutathione-agarose beads, subjected to SDS-PAGE, and visualized by Coomassie Brilliant Blue (*CBB*) staining (*lower panel*). Incorporation of ^{32}P was detected with a PhosphorImager (*upper panel*). *C*, the indicated extracts in *A* were incubated in the presence of no DNA, $(dA)_{70}$-$(dT)_{70}$ (*upper panels*), EcoRI-damaged sperm chromatin (*middle panels*), or aphidicolin (*APH*)-treated chromatin (*lower panels*). In addition, the extracts either lacked or contained caffeine as indicated. Chromatin fractions were isolated from the extracts and processed for immunoblotting with anti-Xmcm2, anti-phospho-Ser^{92} (*P-S92*), and anti-Xorc2 antibodies as indicated.

min in control egg extracts. By contrast, the presence of EcoRI-damaged chromatin elicited a prolonged arrest in interphase. This arrest could be ablated completely by the addition of caffeine. Treatment with EcoRI also caused a major reduction in DNA replication (Fig. 7*B*), consistent with the results of Kobayashi *et al.* (19). The small amount of residual DNA synthesis in EcoRI-treated extracts in comparison with aphidicolin-treated extracts appears to be due to DNA repair because this incorporation was not sensitive to geminin (Fig. 7*C*), which blocks initiation of chromosomal DNA replication. The EcoRI-induced inhibition of replication was almost completely reversed by the addition of caffeine.

To assess the roles of Xatm and Xatr in the inhibition of replication in response to double-stranded DNA breaks, we removed Xatm, Xatr, or both Xatm and Xatr from egg extracts by immunodepletion. As shown in Fig. 7 (*D* and *E*), the removal of either Xatm or Xatr alone resulted in significant restoration of DNA replication in EcoRI-treated extracts (to ~20–30% of the level in mock-depleted extracts lacking EcoRI). Furthermore, depletion of both Xatm and Xatr resulted in a level of DNA replication that was ~70% of the normal level. Therefore, it appears that both Xatm and Xatr act cooperatively to inhibit DNA replication in response to double-stranded DNA breaks.

In principle, Xatm and Xatr could directly regulate one or more targets that are necessary for DNA replication. Another (although not mutually exclusive) possibility is that Xatm and Xatr could initiate this response through activating downstream checkpoint effector kinases (*e.g.* Xchk2 and Xchk1, respectively). However, we observed that immunodepletion of Xchk2, Xchk1, or both Xchk2 and Xchk1 from egg extracts had no effect on the ability of EcoRI to cause inhibition of chromosomal DNA replication in egg extracts (Fig. 7*G*). This observation favors the possibility that Xatm and Xatr exert their inhibitory effects directly or perhaps act through distinct downstream effectors.

To assess the role of Ser^{92} phosphorylation on Xmcm2 by Xatm and Xatr, we added various non-phosphorylatable mutants of baculovirus-expressed Xmcm2 to egg extracts to observe potential dominant-negative effects. We chose this approach because immunodepletion of Xmcm2 from egg extracts results in removal of the entire MCM complex, and functional reconstitution of any vertebrate MCM complex that could be used for add-back experiments has not been reported at this time. We mutated Ser^{92} to either alanine or aspartic acid (to potentially mimic constitutive phosphorylation at this site). We introduced these mutations into both Xmcm2 tagged at the C-terminal end with GST and His_6 (Xmcm2-GST-His_6) and Xmcm2 tagged at the N-terminal end with His_6 (His_6-Xmcm2). The endogenous MCM complex in egg extracts appears to be dynamic in that we could observe association of exogenously added, recombinant Xmcm2 with endogenous MCM subunits. For example, as shown in Fig. 8*A*, we could demonstrate binding of endogenous Xmcm4 and Xmcm7 to the wild-type, S92A, and S92D versions of exogenously added Xmcm2-GST-His_6.

Next, we examined whether the addition of the Ser^{92} mutants of Xmcm2 to egg extracts could have a functional consequence. Since we could express His_6-Xmcm2 in higher amounts than Xmcm2-GST-His_6 in insect cells, we pursued using His_6-tagged proteins for these experiments. We added wild-type His_6-Xmcm2, His_6-Xmcm2(S92A), or His_6-Xmcm2(S92D) to egg extracts at a level ~6-fold over that of endogenous Xmcm2. We found that all three recombinant proteins could associate with chromatin to equal extents (Fig. 8*B*). This observation is consistent with the finding that recombinant Xmcm2 can associate with other MCM subunits (*e.g.* Xmcm4 and Xmcm7). The recombinant Xmcm2 proteins on chromatin could be distinguished on the basis of a slightly slower electrophoretic mobility due to the presence of the His_6 tag. However, none of these

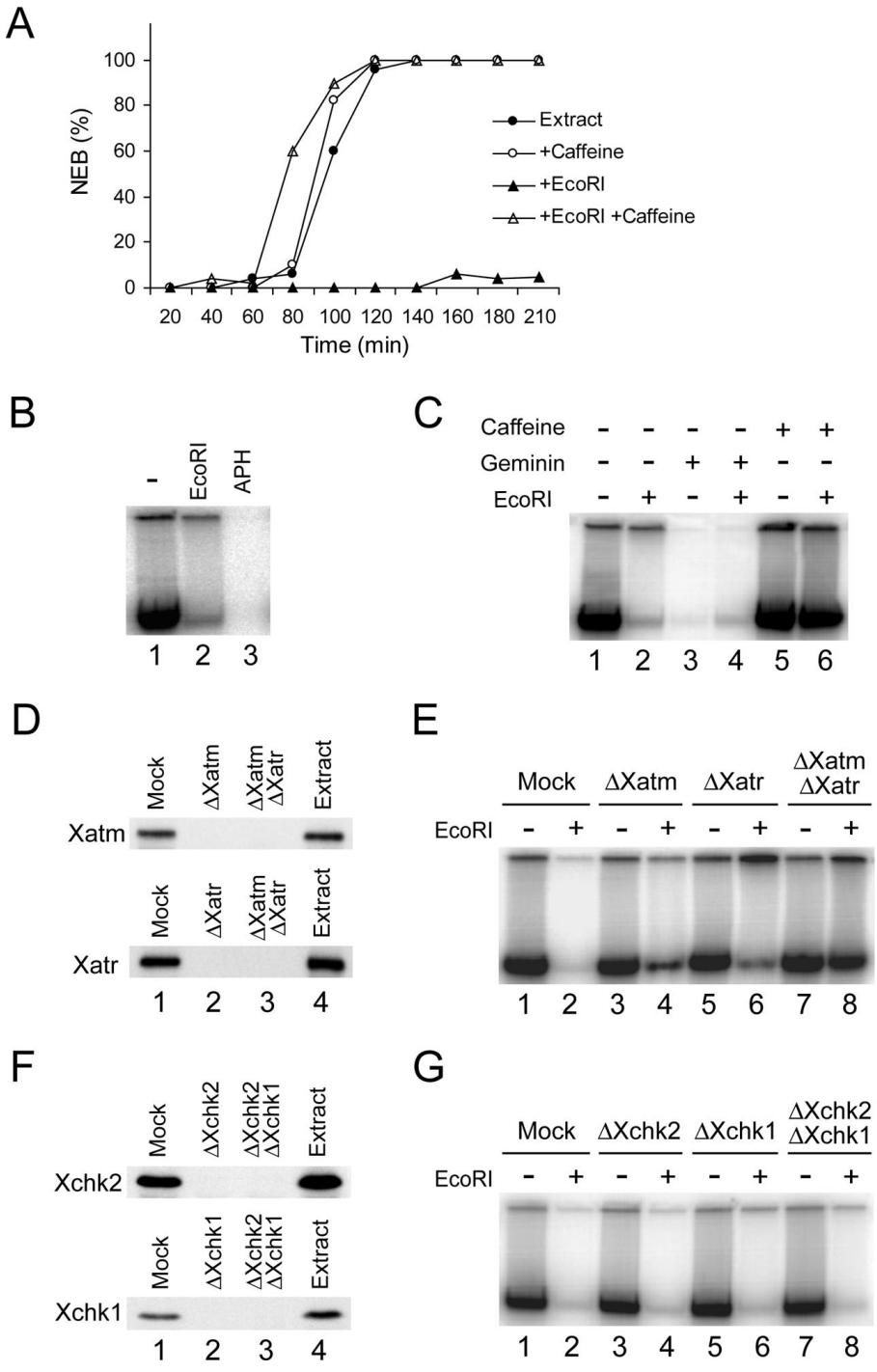

FIG. 7. **DNA replication is inhibited by double-stranded DNA breaks in an Xatm- and Xatr-dependent manner.** *A*, interphase extracts containing sperm nuclei (1000/μl) were incubated with no drug (●), caffeine (○), EcoRI (▲), or EcoRI plus caffeine (△) as indicated. Nuclear envelope breakdown (*NEB*) was determined at the indicated times by microscopy. *B*, shown is the DNA replication of sperm chromatin. Interphase extracts containing sperm nuclei were incubated for 90 min with no drug (*lane 1*), EcoRI (*lane 2*), or aphidicolin (*APH*) (*lane 3*). Incorporation of ^{32}P from [^{32}P]dATP into chromatin was detected with a PhosphorImager. *C*, inhibition of replication by EcoRI was reversed by caffeine. Extracts were treated with buffer alone (*lanes 1* and *2*), geminin (*lanes 3* and *4*), or caffeine (*lanes 5* and *6*). Sperm chromatin was incubated in the extracts in the absence (*lanes 1*, *3*, and *5*) or presence (*lanes 2*, *4*, and *6*) of EcoRI. Incorporation of ^{32}P from [^{32}P]dATP into chromatin was detected with a PhosphorImager. *D*, shown is the immunodepletion of Xatm (Δ*Xatm*), Xatr (Δ*Xatr*), or both Xatm and Xatr. Extracts were treated with control IgG (*upper and lower panels*, *lane 1*), anti-Xatm antibodies (*upper panel*, *lane 2*), anti-Xatr antibodies (*lower panel*, *lane 2*), or both anti-Xatm and anti-Xatr antibodies (*upper and lower panels*, *lane 3*) and processed for immunoblotting with anti-Xatm (*upper panel*) or anti-Xatr (*lower panel*) antibodies. *Lane 4* (*upper and lower panels*) depicts untreated extract. *E*, depletion of both Xatm and Xatr rescued the replication arrest induced by double-stranded DNA breaks. Mock-depleted extracts (*lanes 1* and *2*), Xatm-depleted extracts (*lanes 3* and *4*), Xatr-depleted extracts (*lanes 5* and *6*), or Xatm- and Xatr-depleted extracts (*lanes 7* and *8*) were incubated in the absence (*lanes 1*, *3*, *5*, and *7*) or presence (*lanes 2*, *4*, *6*, and *8*) of EcoRI. Incorporation of ^{32}P from [^{32}P]dATP into chromatin was detected with a PhosphorImager. *F*, shown is the immunodepletion of Xchk2 (Δ*Xchk2*), Xchk1 (Δ*Xchk1*), or both Xchk2 and Xchk1. Extracts were treated with control IgG (*upper and lower panels*, *lane 1*), anti-Xchk2 antibodies (*upper panel*, *lane 2*), anti-Xchk1 antibodies (*lower panel*, *lane 2*), or both anti-Xchk2 and anti-Xchk1 antibodies (*upper and lower panels*, *lane 3*) and processed for immunoblotting with anti-Xchk2 (*upper panel*) or anti-Xchk1 (*lower panel*) antibodies. *Lane 4* (*upper and lower panels*) depicts untreated extract. *G*, the indicated extracts from *F* were incubated with sperm nuclei in the absence (*lanes 1*, *3*, *5*, and *7*) or the presence (*lanes 2*, *4*, *6*, and *8*) of EcoRI and then assayed for DNA replication.

recombinant proteins affected DNA replication in control untreated extracts. Moreover, these proteins did not cause any obvious restoration of DNA replication in EcoRI-treated extracts.

DISCUSSION

In this study, we have identified Xmcm2 as a protein that associates specifically with Xatm. We proceeded to show that Xmcm2 underwent phosphorylation at Ser^{92} during checkpoint responses to either damaged or incompletely replicated DNA. In these cases, phosphorylation of Ser^{92} involved both Xatm and Xatr, but to different extents depending on the checkpoint-triggering signal. Moreover, recombinant human ATM and ATR both phosphorylated Ser^{92} very efficiently in cell-free kinase assays. Immunodepletion of both Xatm and Xatr largely abolished the functioning of the checkpoint mechanism that blocks chromosomal DNA replication in egg extracts containing damaged DNA. Taken together, these results indicate that Xmcm2 is a target of the DNA damage and DNA replication checkpoint responses in *Xenopus* egg extracts (Fig. 9). In human cells, MCM4 also undergoes caffeine-sensitive, checkpoint-dependent phosphorylation, but a direct role for ATR was not addressed (37). While this manuscript was in preparation, it was reported that ATM and ATR phosphorylate mammalian MCM2 on a site analogous to the one that we have found in Xmcm2 (38).

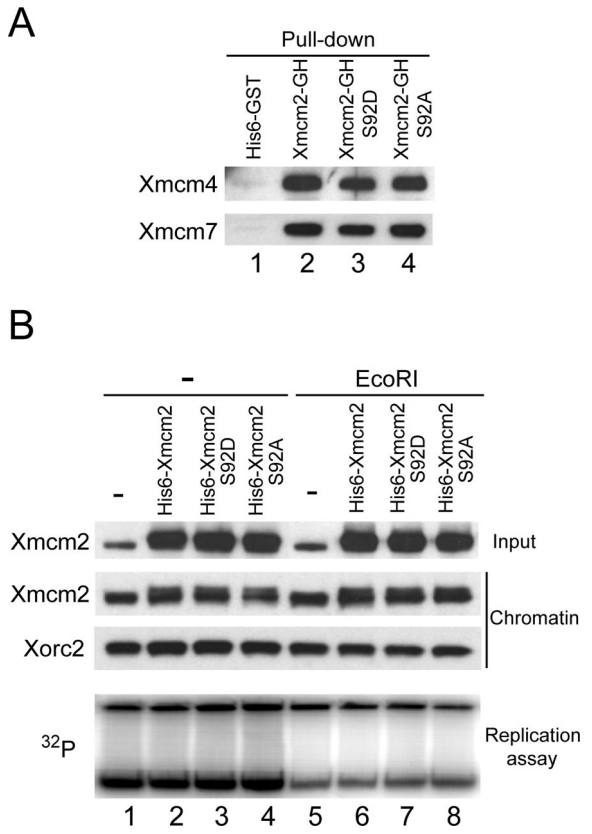

FIG. 8. **Addition of recombinant Xmcm2 with Ser^{92} mutations to *Xenopus* egg extracts.** *A*, recombinant Xmcm2 associated with other MCM subunits in egg extracts. Control His_6-GST, wild-type Xmcm2-GST-His_6 (*Xmcm2-GH*), Xmcm2(S92D)-GST-His_6, and Xmcm2(S92A)-GST-His_6 were incubated in egg extracts and re-isolated with glutathione-agarose beads. The samples were subjected to SDS-PAGE and immunoblotting with anti-Xmcm4 and anti-Xmcm7 antibodies. *B*, egg extracts containing no added protein (*lanes 1* and *5*), wild-type His_6-Xmcm2 (*lanes 2* and *6*), His_6-Xmcm2(S92D) (*lanes 3* and *7*), and His_6-Xmcm2(S92A) (*lanes 4* and *8*) were incubated in the absence (*lanes 1–4*) or presence (*lanes 5–8*) of EcoRI. Whole extracts were immunoblotted with anti-Xmcm2 antibodies (*upper panel*). Chromatin fractions were isolated and immunoblotted with anti-Xmcm2 and anti-Xorc2 antibodies (*middle two panels*). DNA replication was measured by incorporation of ^{32}P from [^{32}P]dATP (*lower panel*).

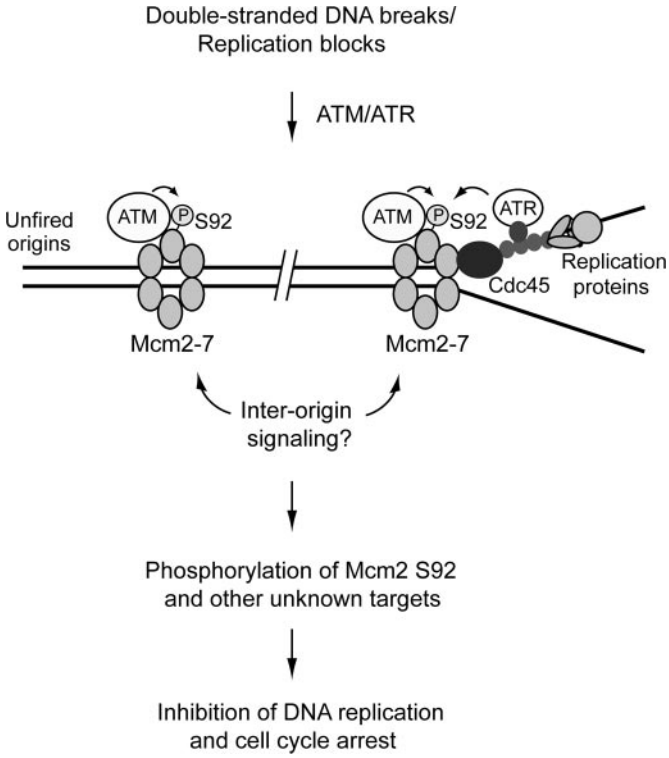

FIG. 9. **Model for inhibition of DNA replication and induction of cell cycle arrest by Xatm and Xatr during checkpoint responses.** See "Discussion" for details.

The MCM complex plays a key role in various aspects of DNA replication (13, 14). This complex is essential for recruiting key replication proteins such as Cdc45 to prospective sites of replication. In turn, Cdc45, along with the kinases Cdk2 and Cdc7, is necessary for the firing of replication origins so that replication protein A and the replicative DNA polymerases can gain access to the unwound DNA. It is now widely accepted that the MCM complex contains a helicase activity that is necessary for replicative unwinding of the DNA, although incontrovertible proof may still be lacking. Altogether, it appears that the MCM complex possesses critical regulatory and catalytic roles in DNA replication. Therefore, this complex would be a logical target for regulating various aspects of DNA replication.

A wide variety of observations have indicated that disruptions in the genome inhibit DNA replication. For example, it is well known that treatment of mammalian cells with ionizing radiation leads to a diminution of DNA replication during S phase. One of the characteristics of ATM-deficient cells is that these cells exhibit "radio-resistant DNA synthesis" following DNA damage (39). This finding implicates ATM as a critical regulator of this normal cellular response to DNA damage. Similarly, in budding yeast, the ATR homolog Mec1 blocks the firing of late replication origins in cells treated with hydroxyurea (40, 41). This pathway appears to inhibit the kinase Cdc7, which is involved in the MCM-dependent loading of Cdc45 onto chromatin in yeast and vertebrates (42, 43).

The checkpoint-dependent inhibition of DNA replication can be studied effectively in *Xenopus* egg extracts. The presence of double-stranded DNA breaks in egg extracts inhibits chromosomal DNA replication as well as entry into mitosis (17–19). Interestingly, aphidicolin, which inhibits DNA polymerase activity, also triggers a pathway that blocks utilization of as yet unfired origins (24, 44). This response is sensitive to the checkpoint-overriding compound caffeine. This sensitivity could be demonstrated by the addition of caffeine to egg extracts containing a concentration of aphidicolin that is sufficient to block subsequent origin firing, but low enough to allow some DNA polymerase activity (24). Under such conditions, treatment with caffeine leads to increased binding of Cdc45 to the DNA and resumed initiation of nascent strand DNA synthesis at newly unwound DNA replication forks. Two different groups have recently extended this observation by demonstrating explicitly that caffeine inhibits ATR and/or ATM in this process (45, 46). We have shown in this work that treatment with aphidicolin led to caffeine-sensitive phosphorylation of Xmcm2 at Ser^{92}. We also found that the suppression of DNA replication in response to double-stranded DNA breaks depended upon both Xatm and Xatr. Previous studies had revealed a role only for Xatm in this pathway (18). Xmcm2 also underwent phosphorylation at Ser^{92} in response to double-stranded DNA breaks in a manner that depended upon both Xatm and Xatr. Overall, although the initiating checkpoint signal appears to be different in both cases (*e.g.* stalled replication forks *versus* double-stranded DNA breaks), phosphorylation of Xmcm2 at Ser^{92} is a shared step of these checkpoint pathways.

In principle, phosphorylation of Xmcm2 at Ser^{92} could have a number of different functions. For example, this phosphorylation could impair the firing of replication origins or limit the helicase activity of MCM complexes at existing replication forks. Either effect would result in diminished DNA replica-

tion. To date, we have not been able to obtain any direct evidence that phosphorylation of Ser^{92} is necessary for DNA damage-dependent inhibition of replication, but it is possible that our methodologies may not be able to detect such an effect. With this caveat, these observations could mean that phosphorylation of Ser^{92} is not necessary for this inhibition or that another inhibitory step(s) acts redundantly with this phosphorylation. Another possibility is that phosphorylation of Ser^{92} may help to stabilize the MCM complex on the chromatin for resumption of DNA replication after repair of checkpoint-inducing lesions. This function may be critical because removal of the MCM complex during S phase irreversibly inhibits recovery from a replication arrest (47). Finally, phosphorylation of Xmcm2 may play some role in the DNA repair process itself.

An interesting property of the MCM complex is that there is a large excess of this complex compared with the amount of the origin recognition complex on chromatin (14, 48, 49). In particular, in *Xenopus* egg extracts, ~10–40 MCM complexes appear to be loaded onto the DNA for each origin recognition complex particle (12). Only a small fraction of these MCM complexes becomes activated for origin firing and DNA unwinding. Such observations illustrate the so-called "MCM paradox," whereby the number of MCM complexes on the DNA greatly exceeds the number of sites for ongoing DNA synthesis. One hypothesis is that an excess of MCM complexes may be critical for ensuring that replication origins are suitably spaced in the genome (see Ref. 12). In addition, a consequence of this apparent surplus is that the MCM complex would be distributed widely on chromatin to respond to any problems or insults in the genome. Significantly, even modestly reduced MCM function confers genomic instability in yeast, which raises the possibility that the MCM complex has a role independent of DNA replication (50). Further study of how ATM and ATR control the replication machinery may help to reveal how vertebrate cells maintain the integrity of their genomes.

Acknowledgments—We are grateful to our colleagues in the laboratory for helpful comments on the manuscript, to Drs. I. M. Ward and J. Chen (Mayo Clinic) for technical advice on the UV filter assay, and to Dr. J. J. Blow for anti-Xmcm4 and anti-Xmcm7 antibodies.

REFERENCES

1. Melo, J., and Toczyski, D. (2002) *Curr. Opin. Cell Biol.* **14,** 237–245
2. Osborn, A. J., Elledge, S. J., and Zou, L. (2002) *Trends Cell Biol.* **12,** 509–516
3. Nyberg, K. A., Michelson, R. J., Putnam, C. W., and Weinert, T. A. (2002) *Annu. Rev. Genet.* **36,** 617–656
4. Abraham, R. T. (2001) *Genes Dev.* **15,** 2177–2196
5. Guo, Z., Kumagai, A., Wang, S. X., and Dunphy, W. G. (2000) *Genes Dev.* **14,** 2745–2756
6. Hekmat-Nejad, M., You, Z., Yee, M., Newport, J. W., and Cimprich, K. A. (2000) *Curr. Biol.* **10,** 1565–1573
7. Liu, Q., Guntuku, S., Cui, X. S., Matsuoka, S., Cortez, D., Tamai, K., Luo, G., Carattini-Rivera, S., DeMayo, F., Bradley, A., Donehower, L. A., and Elledge, S. J. (2000) *Genes Dev.* **14,** 1448–1459
8. Zhao, H., and Piwnica-Worms, H. (2001) *Mol. Cell. Biol.* **21,** 4129–4139
9. Brown, E. J., and Baltimore, D. (2000) *Genes Dev.* **14,** 397–402
10. de Klein, A., Muijtjens, M., van Os, R., Verhoeven, Y., Smit, B., Carr, A. M., Lehmann, A. R., and Hoeijmakers, J. H. (2000) *Curr. Biol.* **10,** 479–482
11. Bell, S. P., and Dutta, A. (2002) *Annu. Rev. Biochem.* **71,** 333–374
12. Edwards, M. C., Tutter, A. V., Cvetic, C., Gilbert, C. H., Prokhorova, T. A., and Walter, J. C. (2002) *J. Biol. Chem.* **277,** 33049–33057
13. Bailis, J. M., and Forsburg, S. L. (2004) *Curr. Opin. Genet. Dev.* **14,** 17–21
14. Forsburg, S. L. (2004) *Microbiol. Mol. Biol. Rev.* **68,** 109–131
15. Dasso, M., and Newport, J. W. (1990) *Cell* **61,** 811–823
16. Kumagai, A., Guo, Z., Emami, K. H., Wang, S. X., and Dunphy, W. G. (1998) *J. Cell Biol.* **142,** 1559–1569
17. Guo, Z., and Dunphy, W. G. (2000) *Mol. Biol. Cell* **11,** 1535–1546
18. Costanzo, V., Robertson, K., Ying, C. Y., Kim, E., Avvedimento, E., Gottesman, M., Grieco, D., and Gautier, J. (2000) *Mol. Cell* **6,** 649–659
19. Kobayashi, T., Tada, S., Tsuyama, T., Murofushi, H., Seki, M., and Enomoto, T. (2002) *J. Cell Sci.* **115,** 3159–3169
20. Kumagai, A., and Dunphy, W. G. (2003) *Nat. Cell Biol.* **5,** 161–165
21. Kumagai, A., and Dunphy, W. G. (2000) *Mol. Cell* **6,** 839–849
22. Coleman, T. R., Carpenter, P. B., and Dunphy, W. G. (1996) *Cell* **87,** 53–63
23. Prokhorova, T. A., and Blow, J. J. (2000) *J. Biol. Chem.* **275,** 2491–2498
24. Yanow, S. K., Gold, D. A., Yoo, H. Y., and Dunphy, W. G. (2003) *J. Biol. Chem.* **278,** 41083–41092
25. Shevchenko, A., Wilm, M., Vorm, O., and Mann, M. (1996) *Anal. Chem.* **68,** 850–858
26. Thomas, H., Havlis, J., Peychl, J., and Shevchenko, A. (2004) *Rapid Commun. Mass Spectrom.* **18,** 923–930
27. Canman, C. E., Lim, D. S., Cimprich, K. A., Taya, Y., Tamai, K., Sakaguchi, K., Appella, E., Kastan, M. B., and Siliciano, J. D. (1998) *Science* **281,** 1677–1679
28. Yoo, H. Y., Kumagai, A., Shevchenko, A., Shevchenko, A., and Dunphy, W. G. (2004) *Cell* **117,** 575–588
29. McGarry, T. J., and Kirschner, M. W. (1998) *Cell* **93,** 1043–1053
30. Mills, A. D., Blow, J. J., White, J. G., Amos, W. B., Wilcock, D., and Laskey, R. A. (1989) *J. Cell Sci.* **94,** 471–477
31. Yan, H., and Newport, J. (1995) *J. Cell Biol.* **129,** 1–15
32. Ward, I. M., Minn, K., and Chen, J. (2004) *J. Biol. Chem.* **279,** 9677–9680
33. Robertson, K., Hensey, C., and Gautier, J. (1999) *Oncogene* **18,** 7070–7079
34. Bakkenist, C. J., and Kastan, M. B. (2003) *Nature* **421,** 499–506
35. Brunn, G. J., Williams, J., Sabers, C., Wiederrecht, G., Lawrence, J. C., Jr., and Abraham, R. T. (1996) *EMBO J.* **15,** 5256–5267
36. Kim, S. T., Lim, D. S., Canman, C. E., and Kastan, M. B. (1999) *J. Biol. Chem.* **274,** 37538–37543
37. Ishimi, Y., Komamura-Kohno, Y., Kwon, H. J., Yamada, K., and Nakanishi, M. (2003) *J. Biol. Chem.* **278,** 24644–24650
38. Cortez, D., Glick, G., and Elledge, S. J. (2004) *Proc. Natl. Acad. Sci. U. S. A.* **101,** 10078–10083
39. Jeggo, P. A., Carr, A. M., and Lehmann, A. R. (1998) *Trends Genet.* **14,** 312–316
40. Shirahige, K., Hori, Y., Shiraishi, K., Yamashita, M., Takahashi, K., Obuse, C., Tsurimoto, T., and Yoshikawa, H. (1998) *Nature* **395,** 618–621
41. Santocanale, C., and Diffley, J. F. (1998) *Nature* **395,** 615–618
42. Weinreich, M., and Stillman, B. (1999) *EMBO J.* **18,** 5334–5346
43. Costanzo, V., Shechter, D., Lupardus, P. J., Cimprich, K. A., Gottesman, M., and Gautier, J. (2003) *Mol. Cell* **11,** 203–213
44. Marheineke, K., and Hyrien, O. (2001) *J. Biol. Chem.* **276,** 17092–17100
45. Marheineke, K., and Hyrien, O. (2004) *J. Biol. Chem.* **279,** 28071–28081
46. Shechter, D., Costanzo, V., and Gautier, J. (2004) *Nat. Cell Biol.* **6,** 648–655
47. Labib, K., Tercero, J. A., and Diffley, J. F. (2000) *Science* **288,** 1643–1647
48. Hyrien, O., Marheineke, K., and Goldar, A. (2003) *BioEssays* **25,** 116–125
49. Laskey, R. A., and Madine, M. A. (2003) *EMBO Rep.* **4,** 26–30
50. Liang, D. T., Hodson, J. A., and Forsburg, S. L. (1999) *J. Cell Sci.* **112,** 559–567